



## Kinetic modeling of a tapered Holweck pump



S. Naris\*, C. Tantos, D. Valougeorgis

Department of Mechanical Engineering, University of Thessaly, Pedion Areos, Volos 38334, Greece

### ARTICLE INFO

#### Article history:

Received 2 February 2014

Received in revised form

26 March 2014

Accepted 4 April 2014

Available online 15 April 2014

#### Keywords:

Knudsen number

Vacuum pumps

Vacuum gas dynamics

### ABSTRACT

The Holweck pump is a device widely used in many pumping systems. It can be a self-standing device or part of a multi-stage system, usually combined with a turbo-molecular pump (TMP). In the present work, an existing methodology [Sharipov et al., 2006] for the simulation of a Holweck pump with channels of constant cross sections, is extended and becomes more general by including pumps with tapered channels. The implemented procedure is based on the kinetic approach, is applicable in the whole range of the Knudsen number and is divided into two steps. First the flow through a tapered channel of a T-shape cross section is decomposed in four simple two-dimensional flows and a database for the dimensionless flow rate in terms of the reference gas rarefaction and the channel geometrical data is built based on linear kinetic theory. Then, using the mass conservation principal and the kinetic database, an ordinary differential equation is solved to yield the pressure evolution along the pump and the pump characteristic quantities of practical interest. Comparison of simulation results with existing experimental data has shown good agreement, proving the validity of the method and its capability of simulating the flow in a Holweck pump with small computational effort. In addition, the great advantage of the method for fast and easy-to-go parametric and sensitivity analysis concerning various operational and geometrical characteristics of the pump is demonstrated.

© 2014 Elsevier Ltd. All rights reserved.

### 1. Introduction

Pumping systems for the creation and maintenance of vacuum conditions is an essential apparatus for many industrial applications. In most cases the systems consist of a high (primary) vacuum pump and a forepump (secondary) which decreases the load of the first, in order to increase its efficiency. One of the most common pumps used as a secondary stage is the Holweck pump [1]. The proper design of such devices is important from both economic and operational point of view.

The Holweck pump belongs to the category of drag pumps which also includes between others the Gaede and the Siegbahn pumps. It is composed by an inner rotating cylinder (rotor) and an outer stationary cylinder (stator). One of them, which is usually the rotor, has spiral guided grooves printed on it, resulting to a gas motion from the high towards the low vacuum port. The depth of the grooves decreases along the printed channels in the flow direction in order to reduce the cross section as pressure and density increase. The operational characteristics of a Holweck pump

depend on several parameters including the geometrical characteristics, the flow parameters (pressure range, temperature, etc.) and the properties of the pumped gas. During the design process, empirical rules are commonly applied for the optimization of the operational characteristics and the adaptation to the application requirements. Manufacturing many prototypes for experimental testing of different configurations is economically inefficient and time consuming. A solid alternative may be the existence of a reliable simulation tool capable to examine different operational and design scenarios fast and with low cost.

When the pump operates in the hydrodynamic or the slip regimes, then it is reasonable to implement the Navier–Stokes equations with or without slip and jump boundary conditions. Using this approach, Sawada and Nakamura [2] have examined the effect of the shape of the channel groove on the performance of the pump, while Cheng et al. [3] have tested both experimentally and computationally a turbo pump including the Holweck stage. Boulon and Mathes [4] have investigated the operation of a Holweck pump using commercial software and compared with experimental data finding good agreement. More recently, Giors et al. [5], also performed both experimental and numerical work and they investigated the viscous and the early-transition regimes. Data presented in that paper [5] are used in the present work for validation of the proposed methodology.

\* Corresponding author.

E-mail addresses: [snaris@mie.uth.gr](mailto:snaris@mie.uth.gr) (S. Naris), [christantos@mie.uth.gr](mailto:christantos@mie.uth.gr) (C. Tantos), [diva@mie.uth.gr](mailto:diva@mie.uth.gr) (D. Valougeorgis).

Simulation tools that can be used when the flow is in a wide range of the Knudsen number include either a hybrid type approach where a continuum and a mesoscale (kinetic) solver are coupled in a computationally efficient manner, or a solely kinetic solver which remains computationally efficient by focusing on a specific application and taking advantage of certain flow characteristics. In this work we are considering the second approach by working on the flow configuration of the Holweck pump.

Simulation of the flow in the Holweck stage via mesoscale modeling tools has attracted considerable attention lately with the stochastic approach being more popular, compared to the deterministic one, due to its simplicity and easy adaptation to more complex geometries. More specifically, the Test Particle Monte Carlo method is used to examine the free molecular flow in a Holweck pump [6], while the Direct Simulation Monte Carlo (DSMC) method is applied in drag pumps for operational conditions where the flow is in the transition and slip regimes [7,8]. In all cases pumps with channels of constant cross section are simulated. The DSMC approach has been proved reliable and accurate for engineering purposes in a wide range of the Knudsen number. Its main drawback is that it can be computationally very time-demanding and that in low Reynolds and Mach numbers its accuracy is reduced drastically due to statistical noise. The deterministic approach based on the solution of the Boltzmann equation has also been used and some results in simplified configurations for demonstration purposes have been reported [9,10]. The fully three-dimensional flow field is simulated resulting to high demands of CPU time and memory requirements. This is a significant disadvantage when different design concepts or operational scenarios have to be tested since the required time and resources might be unacceptable.

To circumvent these pitfalls a simple methodology based on linear kinetic theory with small computational requirements has been proposed in Ref. [11] for the numerical modeling of a Holweck pump. It consists of two steps. In the first step the flow through a pump channel is decomposed in each cross section into four two-dimensional flows and more specifically, in one pressure driven and one boundary driven flow in the longitudinal direction with respect to the main flow as well as to the corresponding ones in the transverse direction. Once the flow rates of these basic flows are computed in terms of the channel cross section and the gas rarefaction, in the second step they are linearly superimposed and through the solution of an ordinary differential equation, which has been derived by fulfilling the mass conservation principal, the pump characteristic quantities of practical interest are calculated. The method is applied only in a single channel and then taking into account the channel periodicity the results are easily adjusted to include all the channels of the pump. Due to its simplicity the methodology is suitable for efficient parametric and sensitivity analysis of all involved parameters in the design and performance optimization of a Holweck pump.

However, the methodology has been applied so far in pumps where the cross section of the channels is assumed to be constant. This may give a rough estimation of the pump characteristics but is not enough for the majority of the industrial devices where the channels have variable cross section and the area is decreased in the flow direction as the pressure in the pump is increased. Actually, this is a weak point of the existing approach and for this reason it has received in the past some criticism [5].

In the present work the methodology introduced in Ref. [11] is extended and becomes more general by including pumps with tapered channels. This is achieved by incorporating in the formulation the variable cross section approach, which has been applied in long tubes and channels [12–14]. The upgraded methodology is implemented to model a tapered Holweck pump and the results are

compared with experimental data available in the literature achieving very good agreement. In addition, simulations are performed for various geometrical and operational parameters and the feasibility of the method for efficient and easy-to-go parametric analysis is demonstrated.

## 2. Channel geometry and flow configuration

Simulation of the exact geometry of the Holweck pump demands a computational domain that includes the pump stage as well as certain volumes in the high vacuum inlet and fore vacuum outlet ports in order to take into account the end effects. Also, the curvature effect has to be included. The consideration of these effects hardens significantly the modeling process. It has been shown however, that when the ratio of the length of the channel over a characteristic length of the cross section (e.g. hydraulic diameter) is large, the end effect can be neglected [15]. Similarly, the curvature effect can be ignored when the radius of the pump is large enough compared to the hydraulic diameter of the pump channels. These conditions are fulfilled for the majority of the Holweck pumps and therefore in the present analysis both effects are not taken into consideration. In addition, a linear treatment may be applied.

The geometry of the channel, shown in Fig. 1(a) is specified by its depth  $H$ , width  $W$  and length  $L_x = L/\sin\gamma$ , where  $L$  is the pump axial length and  $\gamma$  is the angle with respect to the front face of the pump,

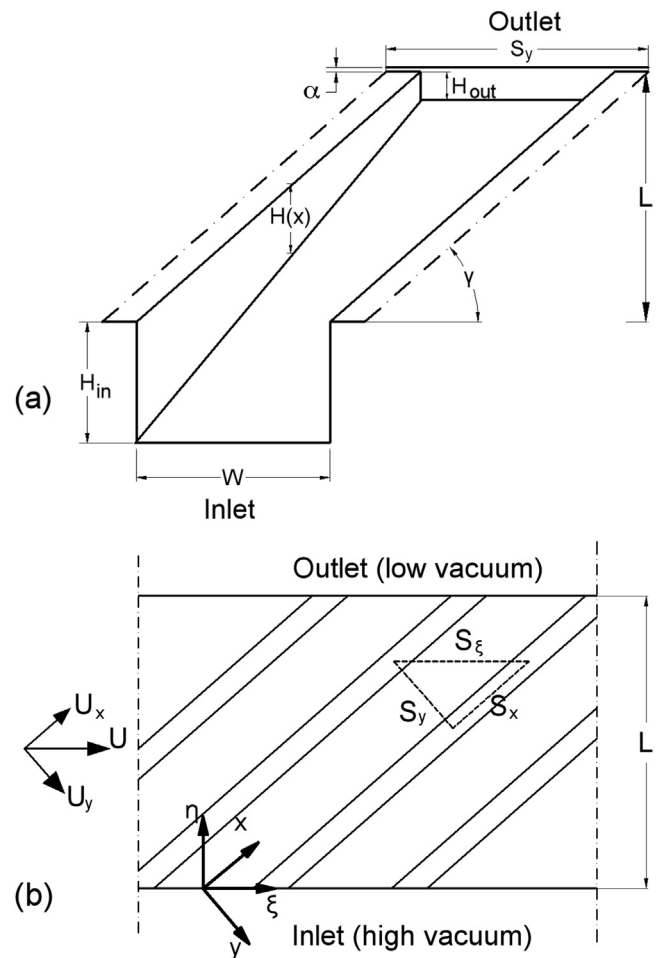


Fig. 1. Configuration of the Holweck pump: (a) geometry of the tapered channels; (b) view of a series of channels with the pump and channel coordinates systems  $(x, y)$  and  $(\eta, \xi)$  respectively.

the clearance between the rotor and the stator  $\alpha$  and the periodicity length  $S_y$ . All quantities are constant except the depth  $H = H(x)$ , which varies linearly in the  $x$ -direction, between the inlet and outlet values denoted by  $H_{in}$  and  $H_{out}$  respectively. It is seen that the cross section of the channel looks like the capital T letter and therefore the terminology T-shape channel in the rest of the manuscript is used. The hydraulic diameter of the cross section defined as  $D_h = 4A/\Gamma$ , where  $A$  and  $\Gamma$  are the area and the perimeter of the cross section, varies along the channel and in terms of the channel dimensions is given by

$$D_h(x) = 2 \frac{S_y \times \alpha + W \times H(x)}{S_y + H(x) + \alpha} \quad (1)$$

with  $D_{h,in}$  and  $D_{h,out}$  denoting the hydraulic diameter at the inlet and outlet of the channel respectively. In the formulation procedure the hydraulic diameter is taken as the characteristic dimension in each T-shape cross section.

In Fig. 1(b) a more general view of a series of few channels is shown. The channel coordinate system  $(x, y)$  with  $x$  and  $y$  denoting the longitudinal and transverse axes with respect to the channel as well as the corresponding pump coordinate system  $(\eta, \xi)$  are also defined. Due to the periodicity in the channel configuration, the flow through only one channel with a T-shape variable cross section is solved. Based on the pump coordinate system the flow field is created by the motion of the upper plate with velocity  $U$  in the  $\xi$  direction and the local pressure gradient  $X_p^\eta$  in the  $\eta$  direction. These quantities are the forcing terms inducing the flow and it is convenient to represent them in terms of the channel coordinate system  $(x, y)$  according to

$$U_x = U \cos(\gamma) \quad U_y = U \sin(\gamma) \quad (2)$$

$$X_p^x = X_p^\eta \sin(\gamma) \quad X_p^y = -X_p^\eta \cos(\gamma) \quad \text{where} \quad X_p^\eta = \frac{D_h}{P} \frac{\partial P}{\partial \eta} \quad (3)$$

where  $U_x$  and  $U_y$  are the velocity components of the moving plate above the channel and  $X_p^x$  and  $X_p^y$  the components of the local pressure gradient in the channel. These four forcing terms induce the following four two-dimensional flows under consideration: (i) longitudinal Couette, (ii) transverse Couette, (iii) longitudinal Poiseuille and (iv) transverse Poiseuille. Due to the linearity of the problem these flows are considered separately and their solutions are superimposed to yield the pump solution. It is noted that the assumption of linearity, is still valid even for large differences between the inlet and outlet pressure of the channel, provided that the ratio of the channel length over the hydraulic diameter is adequately large [17].

A flow quantity of primary importance is the local gas rarefaction parameter  $\delta$ , which is proportional to the reversed Knudsen number and is defined as

$$\delta = \frac{PD_h}{\mu u_0} \quad (4)$$

where  $P = P(x)$ , is the local pressure along the channel, while  $P_{in}$  and  $P_{out}$  denote the inlet and outlet pressure respectively,  $\mu$  is the gas viscosity at reference temperature  $T$  and  $u_0 = \sqrt{2k_B T/m}$  is the most probable velocity, with  $k_B$  denoting the Boltzmann constant and  $m$  the molecular mass. The gas rarefaction parameter varies in the  $x$ -direction along with the hydraulic diameter and pressure. It is noted that the dimensionless flow rates are computed at each cross section in terms of the local geometrical data of the T-shape cross section and the local rarefaction parameter, which however, is not known a-priori and is part of the solution.

### 3. Kinetic modeling procedure

The detailed description of the kinetic modeling process of a Holweck pump is given in Ref. [11]. Therefore here, only parts of the typical formulation are repeated for completeness purposes, while all new material related to the extension of the methodology for modeling a tapered Holweck pump is explicitly included.

Following [11], the mass flow rate in the  $\eta$ -direction, denoted by  $\dot{M}_\eta$ , due to the mass conservation principal, can be expressed as

$$\dot{M}_\eta = G_\eta P_{in} \frac{2D_{h,in}^2}{u_0} = G_\eta P_{in} \frac{2D_h^2}{u_0} \beta^2 \quad (5)$$

where  $\beta$  is the ratio of the inlet over the local hydraulic diameter and is defined as  $\beta = D_{h,in}/D_h$ , while  $G_\eta$  is the dimensionless flow rate. The other quantities in Eq. (5) have been already defined.

A mass flux balance is performed in the triangular element, with sides  $S_x$ ,  $S_y$  and  $S_\xi$ , shown in Fig. 1(b), to deduce [11]

$$\dot{M}_\eta + \dot{M}_y - \dot{M}_x = 0. \quad (6)$$

The mass flux  $\dot{M}_x$  is due to the longitudinal Couette and Poiseuille flows, which are induced by  $U_x$  and  $X_p^x$  respectively, i.e. the  $x$ -components of the driving forces, namely the upper plate velocity and the local pressure gradient. Similarly, the mass flux  $\dot{M}_y$  is due to the corresponding  $y$ -components, which induce the transverse Couette and Poiseuille flows. It is noted that  $\dot{M}_x$  is the useful flow through the channel, while  $\dot{M}_y$  is the flow through the gap between the two cylinders (backflow) and reduces the efficiency of the pump. The mass flow rate in the  $x$ - and  $y$ - directions may be decomposed and rewritten as [11]

$$\dot{M}_x = \dot{M}_x^P + \dot{M}_x^C = \rho u_0 D_h^2 \left[ -X_p^x G_p^x(\delta) + \frac{U_x}{u_0} G_C^x(\delta) \right] \quad (7)$$

$$\dot{M}_y = \dot{M}_y^P + \dot{M}_y^C = \rho u_0 D_h^2 \frac{S_x}{D_h} \left[ -X_p^y G_p^y(\delta) + \frac{U_y}{u_0} G_C^y(\delta) \right] \quad (8)$$

Here,  $\rho$  is the local mass density,  $\delta$  is the local rarefaction parameter calculated based on the local pressure  $P$  and hydraulic diameter  $D_h$ , while  $S_x$  is the distance shown in Fig. 1(b). The quantities  $G_C^x$ ,  $G_p^x$ ,  $G_C^y$  and  $G_p^y$  are dimensionless flow rates corresponding to the four two-dimensional flows under consideration and they are computed by the proper kinetic algorithms. They depend on the local rarefaction parameter  $\delta$  and the specific geometry of the T-shape cross section.

Substituting finally, Eqs. (5), (7) and (8) into Eq. (6) and following some straightforward manipulation the ordinary differential equation describing the evolution of pressure along the pump is deduced:

$$\frac{\partial P}{\partial \eta} = \frac{\sin(\gamma) \left\{ P \frac{U}{u_0} \cos(\gamma) \left[ G_C^x(\delta) - \frac{S_y}{D_h} G_C^y(\delta) \right] - G_\eta P_{in} \beta^2 \right\}}{D_h \left[ \sin^2(\gamma) G_p^x(\delta) + \frac{S_y}{D_h} \cos^2(\gamma) G_p^y(\delta) \right]} \quad (9)$$

Depending on the flow parameters under investigation two scenarios may be implemented. When the inlet pressure and the flow rate are known, then the outlet pressure (or the compression ratio) may be computed by solving Eq. (9) with a typical integration scheme and at the exit of the pump ( $\eta = L$ ) the outlet pressure is recovered. When the inlet and outlet pressures are known then the corresponding flow rate may be computed by introducing an iterative scheme and solving Eq. (9) in each iteration. More specifically, the boundary conditions are set as  $P(0) = P_{in}$  and  $P(L) = P_{out}$ . The quantity  $G_\eta$  is assumed and then Eq. (9) is solved by numerically

integrating in the  $\eta$  direction up to the exit of the pump. The computed outlet pressure is compared to  $P_{out}$  and if necessary the value of  $G_\eta$  is updated and the whole process is repeated upon convergence. Then, it is straightforward to find the mass flow rate  $\dot{M}_\eta$  from Eq. (5). In both scenarios, in each integration step the dimensionless flow rates are obtained from the kinetic database for the local  $\delta$ . It is noted that for  $\beta = 1$ , Eq. (9) is reduced to the corresponding relation for the pump with constant channels cross section given in Ref. [11].

In the case of a constant cross section pump, the flow rates at the kinetic level are obtained in terms of  $\delta$  for only one specific cross section. Here, where the tapered Holweck pump is examined, the flow rates depend on  $\delta$  and on each cross section along the pump. Therefore, the required kinetic database is larger and its exact size depends on the desired accuracy for the pressure distribution and the other pump quantities. When a rough estimation of the pressure range in the pump is possible, then the required range of  $\delta$  foreseen in the database is reduced. Similarly, the number of different T-shape cross sections that must be included in the database depends on how stiff is the variation of the cross section along the channel and on the required accuracy. The introduced interpolation scheme estimating flow rates between the ones included in the database, also influences the accuracy of the results. It is emphasized that a number of parameters, which are important in the design and optimization of the Holweck pump, are not needed in the kinetic computations and in the development of the kinetic database. This allows simulations of various pumping scenarios by using the same database and applying only the second stage of the methodology, i.e., the solution of Eq. (9), which requires few seconds of CPU time on a desktop computer. This fact makes the parametric and sensitivity analysis very efficient.

The present analysis is valid for isothermal flow. If significant temperature variations are included in the flow field then the solution has to take into account more complex phenomena such as temperature driven flows [18,19]. In principal, the information obtained by solving these flows can be included in the proposed methodology reducing however at some degree its versatility and feasibility.

#### 4. Results and discussion

Simulations based on the present methodology have been performed for the single-stage Holweck pump reported in the paper by Giors et al. [5]. The exact geometrical and operational characteristics of this pump are provided in Table 1 and are considered in the present work as the reference parameters. Based on the data of Table 1 it turns out that the average ratio of the channel length over the hydraulic diameter of the cross section for

the mean channel depth is about 60, justifying the implementation of the linear kinetic approach and the choice of neglecting the end effects. Also, the ratio of the radius of the pump over the hydraulic diameter for the mean channel depth is about 15, which means that the curvature effect is small and may also be neglected.

In Section 4.1 the required kinetic database for this pump configuration is presented. Then, these data are used in Section 4.2 to perform a detailed comparison with the computational and experimental results in Ref. [5] in order to validate the proposed approach. Next, in Section 4.3 simulations are performed by varying the geometrical and operational parameters of the reference pump in order to demonstrate the feasibility of the method for efficient and easy-to-go parametric analysis.

##### 4.1. Kinetic database

The kinetic database is built by numerically solving the linear BGK kinetic model equation subject to diffuse boundary conditions at the solid walls and periodic boundary conditions at the open boundaries between the stator and the rotor along the clearance distance. Diffuse-specular boundary conditions is easy to apply but is not included here since the exact value of the accommodation coefficient depends on the specific characteristics of the gas-surface interaction and is not known for the pump under consideration. In any case, the assumption of diffuse boundary conditions can be considered as reasonable, unless special treatment has been applied on the surfaces, which is not expected. The numerical solution is obtained based on the discrete velocity approach which has been successfully applied before [16] and includes the two transverse and the two longitudinal flows. Transverse type flows with exactly the same configuration as the present ones have been solved in Refs. [20,21], where all the details related to the formulation and the numerical scheme are presented along with associated results. Longitudinal flows through channels of various cross sections have been extensively investigated due to their practical interest. The configuration most related to the present work is the longitudinal flow through a rectangular channel presented in Ref. [22]. This formulation has been extended in a straightforward manner to include the flow through a T-shape cross section channel in Ref. [11], where a brief description of the methodology is provided. This same configuration is also solved here for the needs of the present work.

The database includes the flow rates for 24 different values of the rarefaction parameter accordingly distributed covering the free molecular, transitions and slip regimes. For larger values, an extrapolation scheme has been applied, based on the assumption that for  $\delta > 100$  the flow is actually in the viscous regime. In addition, the database includes the flow rates for 6 different T-shape cross sections for groove depths  $H \in [0.75, 3.25]$  mm. It is noted that in the reference pump,  $H_{in} = 3$  mm and  $H_{out} = 1$  mm.

Results of the built kinetic database for each of the four flows under consideration are given in graphical form in terms of  $\delta$  for all six depths in Fig. 2. It is seen that for the pressure driven flows the plotted flow rates have a strong resemblance with the corresponding ones for flows through rectangular channels with the Knudsen minimum in the transition regime and the almost linear profiles in the viscous regime. In the boundary driven flows the flow rates do not vary significantly with  $\delta$ , with a slight increase in the transition regime. Furthermore it is noted that the flow rates of the transverse flows, i.e.,  $G_C^y$  and  $G_P^y$ , usually are at least one order of magnitude smaller than the corresponding ones in the longitudinal direction for the same rarefaction, since they refer to the flow through the gap between the stator and the rotor which should be as small as possible.

**Table 1**  
Parameters of the tested Holweck pump configuration.

<b>Geometrical parameters</b>	
Pump length ( $L$ )	90 mm
Pump diameter ( $D$ )	90 mm
Groove width ( $W$ )	8.1 mm
Inlet groove depth ( $H_{in}$ )	3.0 mm
Outlet groove depth ( $H_{out}$ )	1.0 mm
Clearance of the pump ( $\alpha$ )	0.25 mm
Angle of channels ( $\gamma$ )	30°
Periodicity length ( $S_y$ )	10.1 mm
Number of grooves on the rotor ( $N$ )	14
<b>Operational parameters</b>	
Rotational frequency ( $f$ )	928 Hz
Gas/pump temperature ( $T$ )	300 K
Pumped gas	N <sub>2</sub>

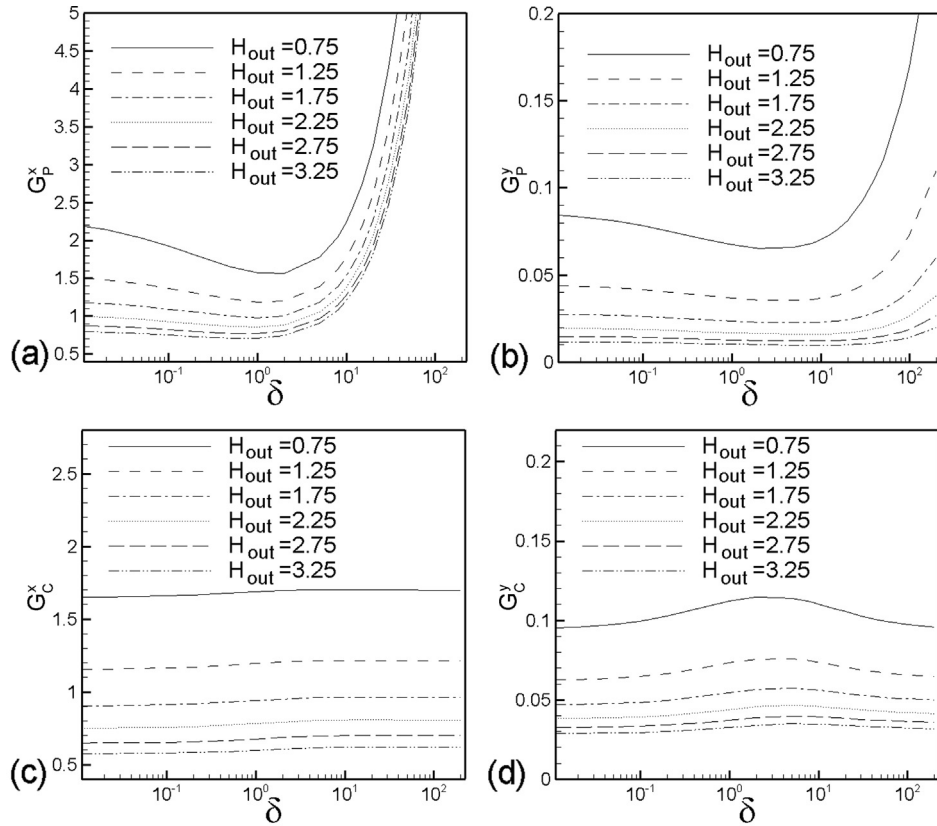


**Fig. 2.** Dimensionless flow rates for the four basic flows through various T-shape channels: (a) longitudinal Poiseuille flow; (b) transverse Poiseuille flow; (c) longitudinal Couette flow; (d) transverse Couette flow.

4.2. Validation on the method

To check the validity of the proposed methodology a comparison with some of the results presented in Ref. [5] is performed for the specific Holweck pump described in Table 1. In Figs. 3 and 4, the inlet versus the outlet gas rarefaction parameter are plotted with

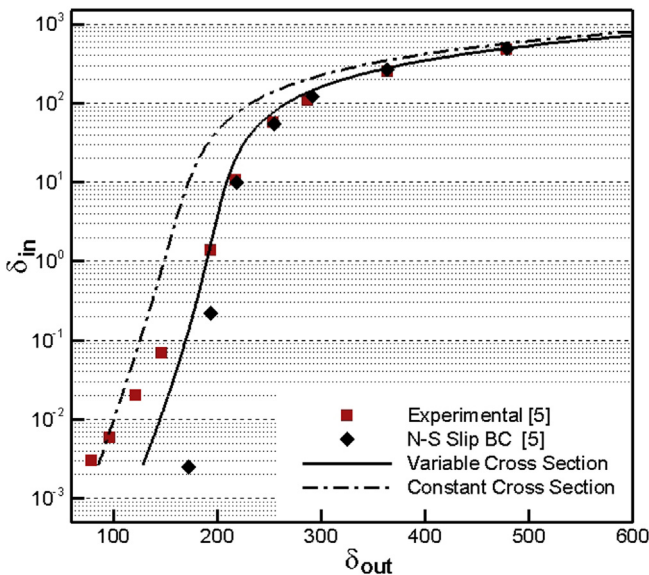


**Fig. 3.** Outlet vs inlet rarefaction parameter for zero gas flow.

zero gas flow and constant gas flow of 250 SCCM (standard cubic centimeters per minute) respectively.

It is seen in Fig. 3 that for the zero flow rate case the agreement between the results obtained by the present analysis of the tapered Holweck pump and the experimental and Navier–Stokes with slip/jump boundary conditions results reported in Ref. [5] is very good. More specifically, the agreement is excellent at large values of  $\delta$  and then as the flow becomes more rarefied and  $\delta$  is decreased there are some deviations. It is seen however, that the present results are in better agreement with the experimental ones compared to the Navier–Stokes results. These observations are according to the range of validity of the extended hydrodynamics theory. The corresponding plots for a constant flow rate of 250 SCCM are given in Fig. 4. Again, the agreement between the results is very good in a wide range of  $\delta$ . There is a small deviation of 10% between the present analysis results and the corresponding experimental ones at small values of  $\delta_{in}$ .

In both cases, discrepancies from experimental results can be partially contributed to the approximations introduced by the linear kinetic modeling approach. More specifically, since the upstream and downstream domains are not considered in the computational scheme, an overestimation of the pressure difference is expected due to the end effects that are not taken into account. It has been observed in Ref. [5] that the pressure increase between the two ends of the pump (which is the one computed by the present approach) is larger than the one in the two domains due to the local pressure drop at the suction (entrance) and discharge (exit) of the pump. Furthermore, in the case of flow rate of 250 SCCM, for small values of  $\delta$ , the density is drastically reduced and consequently the local velocity of the gas is significantly increased in order to keep the fixed flow rate. As a result, the local

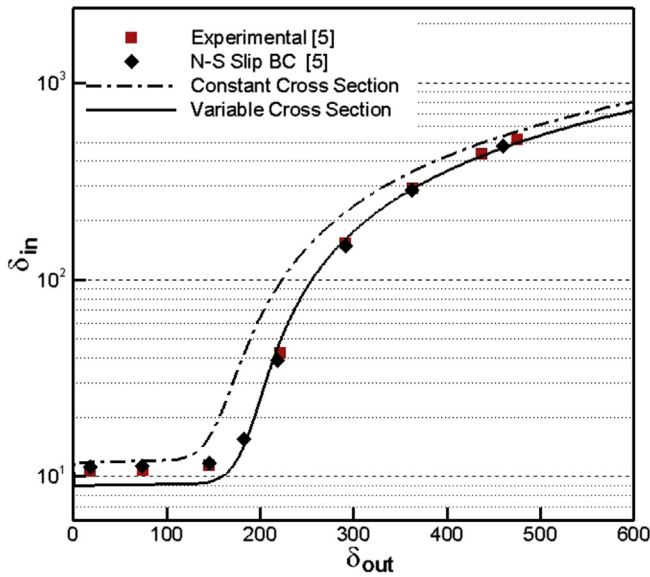


Fig. 4. Outlet vs inlet rarefaction parameter for constant gas flow (250 SCCM).

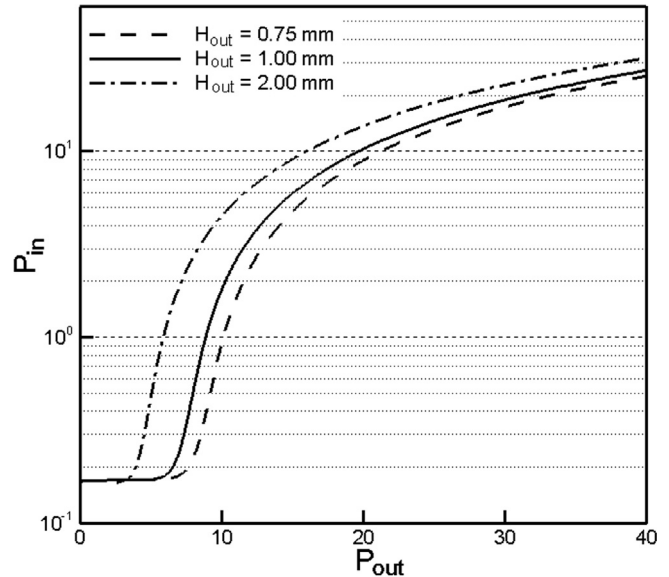


Fig. 5. Outlet vs inlet pressure (mbar) for various values of the outlet channel depth  $H_{out}$ .

Mach number is increased and the accuracy of the linear approach is reduced.

A major issue is to examine the validity of the kinetic methodology of constant cross section in the case of a tapered Holweck pump. Therefore the corresponding results for T-shape channel of constant cross section with an average depth equal to  $(H_{in} + H_{out})/2$  have also been included in Figs. 3 and 4. It is clearly seen that, even though there is acceptable qualitative agreement, in both cases of zero and constant flow rates there are significant discrepancies when the kinetic analysis with the constant cross section is applied. This finding clearly indicates that the kinetic modeling work for the tapered Holweck pump presented here is important and provides a solid supplement to the previous work presented in Ref. [11].

4.3. Sensitivity analysis of design parameters

Typical examples of the parametric analysis that can easily be performed by the proposed approach are given. More specifically, the effect on the pump characteristics of the channel depth and length is shown in Figs. 5 and 6 and of the pump rotational speed and operation temperature in Figs. 7 and 8, while various types of pumped gases are examined in Fig. 9. In all cases, the scenario examined by Giors et al. [5] where the flow rate is set equal to 250 sccm is considered as the reference operation scenario. The influence of each parameter is examined in terms of the inlet and outlet pressure by varying this parameter and keeping the remaining ones unchanged. Also, examples of pump characteristic curves are presented in Fig. 10. All results are based on the kinetic database, given in Section 4.1 and they are recovered in a few seconds on a typical PC.

In Fig. 5, the dependence of the flow on the outlet depth  $H_{out}$  of the channel is given. In all cases  $H_{in} = 3$  mm and the depth is linearly decreased in the flow direction. In addition to the reference parameter  $H_{out} = 1$  mm the cases of  $H_{out} = 0.75$  mm and 2 mm are examined. It is seen that as  $H_{out}/H_{in}$  is decreased, the outlet pressure is increased. This has been also observed in Ref. [5]. In addition, the increase for the outlet pressure is much more significant when the outlet depth is decreased from 2 mm to 1 mm rather than when it is reduced from 1 mm to 0.75 mm. Thus, finding the optimum value depending on the pump input data is a field where the present approach could be very helpful.

In Fig. 6, the influence of the axial pump length  $L$ , is given. It is noted that this length is directly connected to the channel length according to  $L_x = L/\sin\gamma$ , with  $\gamma$  remaining constant. In addition to the reference length  $L = 90$  mm, the cases of  $L = 70$  mm and 110 mm are examined. It is seen that as the length of the pump is increased the outlet pressure is increased, which is expected. At small values of the input pressure, the range of the outlet pressure corresponding to an almost constant inlet pressure is wider as the length increases, due to the increased compression capability of the pump.

The influence of the rotational frequency is shown in Fig. 7, where in addition to the reference frequency of  $f = 928$  Hz, two other scenarios are examined, with  $\pm 20\%$  variation with respect of the reference frequency. The rotational frequency is incorporated in Eq. (9) through the velocity of the upper plate as  $U = \pi Df$ . It is seen that variations of the rotational frequency can result to significant

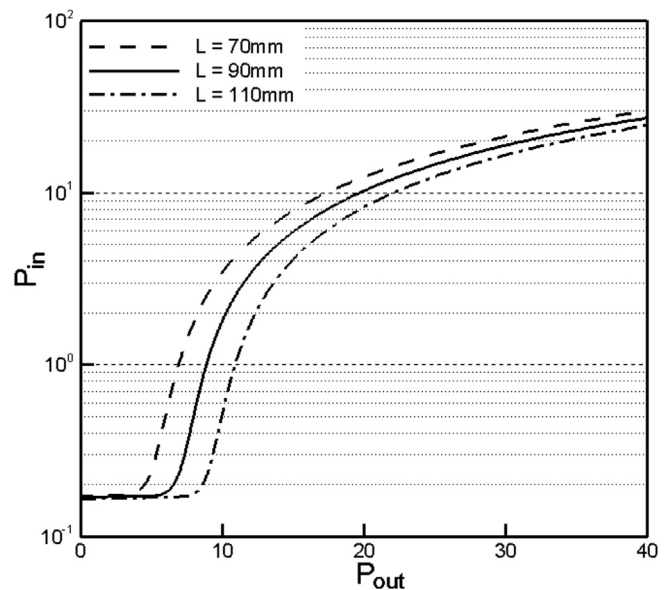


Fig. 6. Outlet vs inlet pressure (mbar) for various values of the pump axial length  $L$ .

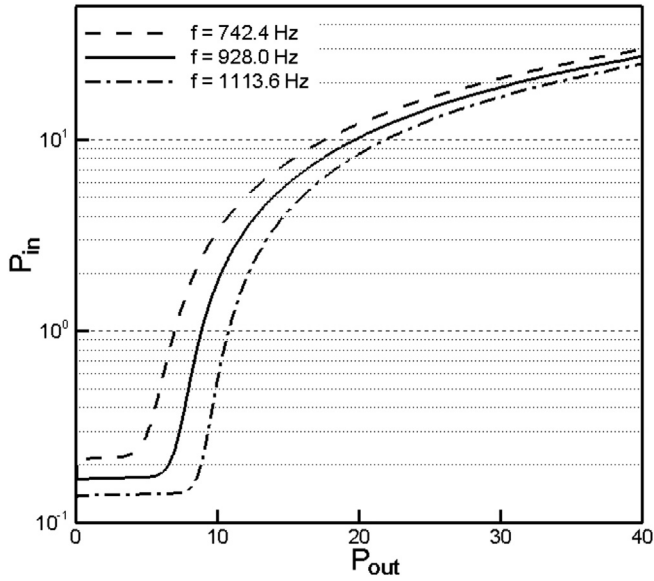


Fig. 7. Outlet vs inlet pressure (mbar) for various values of the pump rotational frequency  $f$ .

changes on the pump operation that extend in the whole spectrum of the pressure values.

The effect of the operation temperature  $T$  is demonstrated in Fig. 8, where the inlet versus the outlet pressure is plotted for  $T = 150, 200, 250$  and  $300$  K. It is assumed that the temperature remain constant throughout the pumping domain. As the temperature is decreased the value of the inlet pressure where the pump operation is initiated is decreased. Also, for constant inlet pressure as the temperature is decreased the outlet pressure is decreased. Thus, in general, the pump performance for the case of a constant flow rate deteriorates at lower temperatures. This effect is important in rarefied conditions, while in the viscous regime is almost vanishing.

The operation characteristics of the pump for various pumped gases, namely He, Ne,  $N_2$  and Ar, are given in Fig. 9. As it is pointed

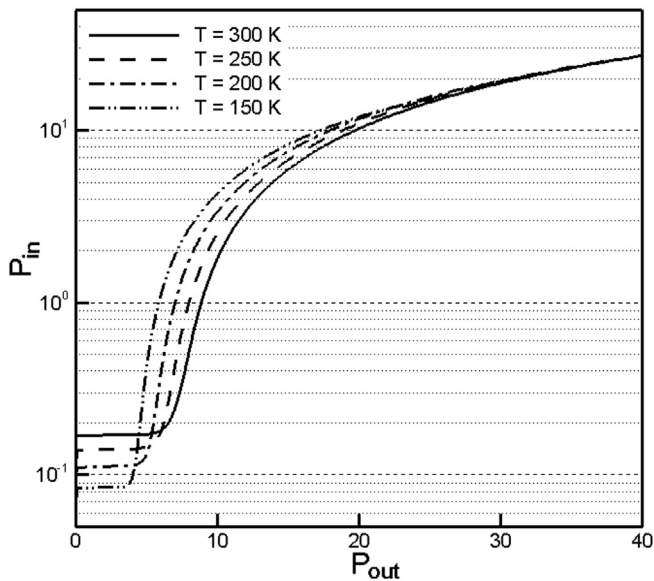


Fig. 8. Outlet vs inlet pressure (mbar) for various values of the pump operation temperature  $T$ .

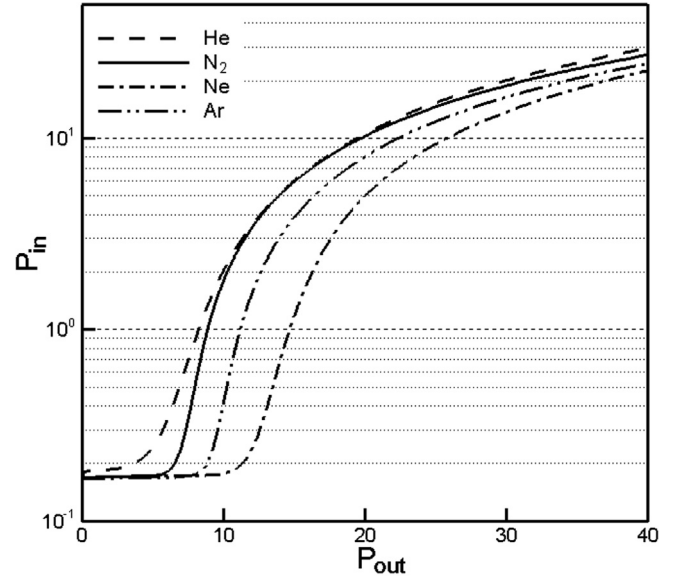


Fig. 9. Outlet vs inlet pressure (mbar) for various pumped gases.

before, in all cases the flow rate is constant and equal to 250 SCCM. It is clearly seen that in general there are large deviations between the corresponding results. For a given input pressure, the output pressure for He and  $N_2$  is about the same, for Ar is larger and for Ne is further increased. This trend is about the same in a wide range of the input pressure. The differences are more evident in more rarefied conditions (lower input and output pressure). At this point it is noted that each gas is defined by its molecular mass and viscosity and thus the observed differences in the results of the inlet versus outlet pressure are contributed to the properties of each gas given in Table 2. Observing carefully the compression ratio of each gas as well the values in Table 2, it is seen that the compression ratios of He and  $N_2$  is very close, while their molecular masses differ significantly and their viscosities are similar. Also, the compression ratios of Ne and Ar are quite apart, while their molecular masses are

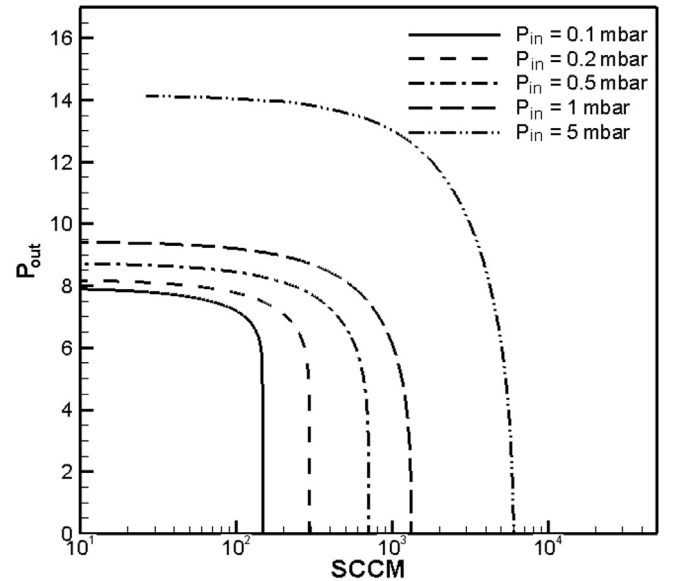


Fig. 10. Pump characteristic curves for various values of the inlet pressure (all other parameters are according to the reference scenario).

**Table 2**  
Properties of gases under investigation.

Gas	Viscosity $\mu$ , (Pa s)	Molecular mass $m$ , (g/mol)
He	$1.99 \times 10^{-5}$	4.0026
Ne	$3.18 \times 10^{-5}$	20.1797
N <sub>2</sub>	$1.79 \times 10^{-5}$	28.0134
Ar	$2.26 \times 10^{-5}$	39.948

close and their viscosities differ significantly. Thus, it may be concluded that in the case of pumping various gases, the gas viscosity plays a more important role compared to its molecular mass in the pump performance.

Finally, some typical characteristics of pump operation for various values of the inlet pressure are provided in Fig. 10. The limiting values of the pump operation parameters are clearly seen. As expected, increase of the inlet pressure results to increased outlet pressure, while the outlet pressure remains almost the same in a wider range of the flow rate.

A general statement, which is deduced from all results presented is that the pump performance is more sensitive to the variation of all parameters examined when the inlet and outlet pressure is reduced. Consequently, sensitivity analysis becomes quite important when the pump operates in the transition rather than in the viscous regime. The presented results are indicative for demonstrating the effectiveness of the proposed methodology and a wider range or even other geometrical and operation parameters can be also treated in a similar manner.

## 5. Concluding remarks

An existing kinetic tool for the simulation of the Holweck pump has been extended to include the more realistic geometry of pumps with tapered channels. The upgraded methodology has been validated by comparison with experimental and numerical results available in the literature. The feasibility of the proposed approach for fast and easy-to-go parametric and sensitivity analysis concerning various operational and geometrical characteristics of the pump has been demonstrated. Furthermore, due to its kinetic origin, the presented approach is capable to accurately simulate the operation of the pump even when part of the flow in the Holweck pump is in the transition regime with very small computational effort.

## Acknowledgments

Part of this work has been supported by the European Communities under the contract of Association EURATOM-Hellenic

Republic within the framework of the EFDA GOT program VACU-TEC (Vacuum Technologies and Pumping). The views and opinions expressed herein do not necessarily reflect those of the European Commission.

## References

- [1] Holweck F. Pompe moléculaire hélicoïdale. *Comptes rendus l'Académie Sci* 1923;43:117.
- [2] Sawada T, Nakamura M. Spiral grooved visco-vacuum pumps with various groove shapes. *Vacuum* 1990;41(7–9):1833–6.
- [3] Cheng HP, Jou RY, Chen FZ, Wang YW, Iwane M, Hanaoka T. Three-dimensional flow analysis of spiral-grooved turbo booster pump in slip and continuum flow. *J Vac Sci Technol A* 2000;18(2):543–51.
- [4] Boulon O, Mathes R. Flow modelling of a Holweck pump stage in the viscous regime. *Vacuum* 2001;60:73–83.
- [5] Giors S, Colombo E, Inzoli F, Subba F, Zanino R. Computational fluid dynamic model of a tapered Holweck vacuum pump operating in the viscous and transition regimes. I. Vacuum performance. *J Vac Sci Technol A* 2006;24(4):1584–91.
- [6] Skovorodko P. Free molecular flow in the Holweck pump. *Rarefied gas dynamics-2000*. In: Bartel TJ, Gallis MA, editors. 22nd International symposium proceedings, AIP conference proceedings, vol. 585; 2001. pp. 900–2.
- [7] Heo JS, Hwang YK. Molecular transition and slip flows in the pumping channels of drag pumps. *J Vac Sci Technol A* 2000;18(3):1025–34.
- [8] Hwang YK, Heo JS. Three-dimensional rarefied flows in rotating helical channels. *J Vac Sci Technol A* 2001;19(2):662–72.
- [9] Kloss YY, Martynov DV, Cheremisin FG. Computer simulation and analysis of the Holweck pump in the transient regime. *Tech Phys* 2012;57(4):451–6.
- [10] Anikin YA, Dodulad OI, Kloss YY, Martynov DV, Shuvalov PV, Tcheremissine FG. Development of applied software for analysis of gas flows in vacuum devices. *Vacuum* 2012;86:1770–7.
- [11] Sharipov F, Fahrenbach P, Zipp A. Numerical modelling of the Holweck pump. *J Vac Sci Technol A* 2005;23(5):1331–9.
- [12] Graur I, Ho MT. Rarefied gas flow through a long rectangular channel of variable cross section. *Vacuum* 2014;101:328–32.
- [13] Sharipov F, Bertoldo G. Rarefied gas flow through a long tube of variable radius. *J Vac Sci Technol A* 2005;23(5):1331–9.
- [14] Tantos C, Naris S, Valougeorgis D. Gas separation in rarefied binary gas mixture flows through long tapered microchannels. In: *Proceedings of 10th HSTAM International congress on mechanics*, Chania, Greece; 2013.
- [15] Pantazis S, Valougeorgis D. Rarefied gas flow through a cylindrical tube due to a small pressure difference. *Eur J Mech B/Fluids* 2013;38:114–27.
- [16] Sharipov F, Seleznev V. Data on internal rarefied gas flows. *J Phys Chem Ref Data* 1998;27(3):657–706.
- [17] Sharipov F, Seleznev V. Rarefied flow through a long tube at any pressure ratio. *J Vac Sci Technol A* 1994;12(5):2933–5.
- [18] Ritos K, Lihnaropoulos J, Naris S, Valougeorgis D. Pressure and temperature driven flows through triangular and trapezoidal microchannels. *Heat Transf Eng* 2011;32:1101–7.
- [19] Pantazis S, Naris S, Tantos C, Valougeorgis D, Andre J, Millet F, et al. Nonlinear vacuum gas flow through a short tube due to pressure and temperature gradients. *Fusion Eng Des* 2013;88(9–10):2384–7.
- [20] Naris S, Valougeorgis D. Boundary driven non-equilibrium gas flow in a grooved channel. *Phys Fluids* 2007;19:067103.1–067103.15.
- [21] Naris S, Valougeorgis D. Gas flow in a grooved channel due to pressure and temperature. In: *Proceedings of ASME 4th International conference on nanochannels, microchannels and minichannels*, Limerick, Ireland; 2006.
- [22] Sharipov F. Rarefied gas flow through a long rectangular channel. *J Vac Sci Technol A* 1999;17(5):3062–6.